

Micellar morphological transformations for a series of linear diblock model surfactants

Asfaw Gezae Daful and Allan D. Mackie

Citation: *The Journal of Chemical Physics* **140**, 104905 (2014); doi: 10.1063/1.4867894

View online: <http://dx.doi.org/10.1063/1.4867894>

View Table of Contents: <http://scitation.aip.org/content/aip/journal/jcp/140/10?ver=pdfcov>

Published by the [AIP Publishing](#)

Articles you may be interested in

[Interaction of photosensitive surfactant with DNA and poly acrylic acid](#)

J. Chem. Phys. **140**, 044907 (2014); 10.1063/1.4862679

[Monte Carlo simulations for amphiphilic aggregation near a water phase transition](#)

J. Chem. Phys. **131**, 144901 (2009); 10.1063/1.3244676

[Orientational bonding model for temperature dependent micellization and solubility of diblock surfactants](#)

J. Chem. Phys. **131**, 114901 (2009); 10.1063/1.3227905

[The interactions between surfactants and vesicles: Dissipative particle dynamics](#)

J. Chem. Phys. **130**, 245101 (2009); 10.1063/1.3155209

[Sphere-to-rod transitions of micelles in model nonionic surfactant solutions](#)

J. Chem. Phys. **118**, 3816 (2003); 10.1063/1.1539048



AIP | Journal of
Applied Physics

Journal of Applied Physics is pleased to
announce **André Anders** as its new Editor-in-Chief

Micellar morphological transformations for a series of linear diblock model surfactants

Asfaw Gezae Dafu¹ and Allan D. Mackie^{2,a)}

¹*School of Chemical and Bio Engineering, Addis Ababa Institute of Technology, Addis Ababa University, P.O. Box 385, Addis Ababa, Ethiopia*

²*Departament d'Enginyeria Química, ETSEQ, Universitat Rovira i Virgili, Av. dels Països Catalans 26, 43007 Tarragona, Spain*

(Received 9 November 2013; accepted 12 February 2014; published online 12 March 2014)

The concentration induced shape transitions of linear model surfactants, H_xT_y , on a lattice have been studied using Monte Carlo simulation. It has been found that a sphere to cylinder shape transition is generally found on shortening the hydrophilic part of the surfactant and anticipates an eventual phase transition. Asymmetric surfactants with longer heads than tails ($x > y$) prefer to form only spherical micelles independent of total surfactant concentration while asymmetric surfactants with longer tails than heads ($x < y$) form spherical micelles at lower concentration and undergo a shape transition to cylindrical micelles on increasing the total concentration. Finally, in the case of symmetric surfactants with $x = y$, only the shortest surfactants H_1T_1 and H_2T_2 undergo a sphere to cylinder shape transition on increasing surfactant concentration. Longer symmetric surfactants are always found to prefer to form spherical micelles. © 2014 AIP Publishing LLC. [<http://dx.doi.org/10.1063/1.4867894>]

I. INTRODUCTION

In order to fully exploit the properties of micellar systems so that they can be controlled and designed for specific purposes, a detailed understanding of their formation is required. Such an understanding needs to be based on an explicit microscopic description of the system; however, fully deterministic predictions of self-assembly in closed systems are rare.¹ One of the many interesting features of micelles is their ability to assume different geometrical forms and even transform from one form to another on changing the experimental conditions. Experimentally, Debye and Anacker² and Eriksson and Ljunggren³ showed that micelles can undergo a transition from spherical to rod-like aggregates upon increasing surfactant concentration above the critical micelle concentration, or CMC. This idea has been supported by many other experimental works.⁴⁻⁹ From a modeling perspective, several studies using both Monte Carlo simulations¹⁰⁻¹⁶ and molecular dynamics^{17,18} have specifically focused on aspects of the micellar sphere to rod transition. Furthermore, mean field theories have also been used to study the same transition.¹⁹⁻²¹ In our recent paper,²² a detailed study was performed for the shape transitions of micelles of model surfactants H_3T_6 and H_4T_4 via two dimensional Single Chain Mean Field Theory (SCMFT) and Monte Carlo simulations. The symmetric surfactant H_4T_4 was found to prefer to form spherical micelles while the asymmetric surfactant H_3T_6 was observed to undergo transitions from spheres to cylinders.

In the present article, three dimensional Monte Carlo simulations are presented for a lattice model to extend the previous work²² for just two surfactants to study the micellar shape transitions of a series of model surfactants, H_xT_y ,

as a result of changing the concentration of surfactants in the system. The main purpose being to present a detailed exploration of concentration dependent shape transitions for non-ionic surfactant aggregates as a function of the lengths of the hydrophobic and hydrophilic blocks. This contribution uses information about the micellization behavior of these surfactants from a work by Floriano *et al.*²³ where it was shown that surfactants from this simple lattice model with just one independent interaction parameter display either macroscopic phase separation or micellization, but not both. Indeed, in their paper they mention that close to this boundary between phase separation and micellization that there is a tendency to form elongated micellar structures. Here we will make a detailed exploration of this region to try and quantify this behavior. The temperatures used for each system are also taken from this reference where possible and are sufficiently low to allow for a clear separation of the micelles from the free chains in the aggregate size distributions. In addition, a Single Chain Mean Field Theory will be used to analyze in greater detail the free energies of the micelles as they change form. The SCMFT is able to calculate the free energies with a very high precision and gives complementary information to the Monte Carlo simulations.

The paper is organized as follows. In Sec. II the lattice model is described followed by Secs. III and IV where details of the Monte Carlo simulations and an overview of the SCMFT are specified, respectively. This is followed by Sec. V which is devoted to an analysis of the results. Finally, the paper finishes with Sec. VI, where the main conclusions are given.

II. THE MODEL

A lattice model is used in this work for nonionic surfactants, originally proposed by Larson.²⁴ In particular, a cubic

^{a)} Author to whom correspondence should be addressed. Electronic mail: allan.mackie@urv.cat

lattice of $L \times L \times L$ sites completely occupied by either solvent or surfactant is chosen. Each solvent molecule, S, occupies one lattice site while the linear amphiphilic molecules, H_xT_y , occupy a set of connected sites, where H and T are the hydrophilic head and hydrophobic tail units, respectively, and x and y represent the number of segments in the head and tail groups. Every lattice site is connected to its $z = 26$ nearest or diagonally nearest adjacent cells, all of which are considered to be neighbors. The interaction energy of a site belonging to a solvent monomer or the head of a surfactant with another type solvent or head site is ϵ_{HH} . An interaction occurs when two sites are neighbors. The tail-tail and head-tail interaction energies are ϵ_{TT} and ϵ_{HT} , respectively. It can be shown that there is only one relevant energy parameter due to the lattice conservation equations, namely $\epsilon = \epsilon_{HT} - \frac{1}{2}(\epsilon_{HH} + \epsilon_{TT})$, from which we define the dimensionless temperature, $T^* = k_B T / \epsilon$.

III. MONTE CARLO SIMULATION

Standard periodic boundary conditions were imposed in all dimensions to mimic an infinite size system. The simulations were initiated with a random configuration and 10^9 Monte Carlo steps were applied in order to make sure that the systems were equilibrated. An additional 5×10^{10} steps were then used in order to calculate the average properties of the system. Chain reptations (80%), a configurational bias Monte Carlo move for chain regrowth (19.99%) and cluster moves (0.01%), are used in this work to sample phase space in an efficient manner.²⁵ In this article, a cluster is defined when surfactants have at least one contact between their tail segments. The three principal radii of gyration of the clusters with more than 10 surfactants, $R_{1,2,3}$, were calculated, and ordered from largest to smallest so that $R_1 > R_2 > R_3$. These values give an idea of the size and shape of the micelle. We also define two ratios of the radii of gyration as follows: $\alpha = (R_2/R_1)^2$ and $\beta = (R_3/R_1)^2$, which give information about the shape of the cluster.²² Note that, by definition, α and β have values in the range (0, 1). If both α and β are close to unity, this implies that the aggregate is approximately spherical. If α and β are close to zero, the aggregate has a cylindrical shape. Finally, if $\alpha \approx 1$ and $\beta \approx 0$ the aggregate will be discoidal. In Sec. V, we will use plots of α and β in order to identify shape transitions in the micellar systems.

IV. SINGLE CHAIN MEAN FIELD THEORY

The Single Chain Mean Field Theory is a mean-field approach that uses configurations of single chains, placed in a mean-field.^{19,26-28} In this work, a two dimensional version of the SCMFT presented in our previous work^{22,29} was used where the mean field is divided into slices or layers along the z -axis and concentric shells of radii r in the x - y plane of the simulation box, as shown in Fig. 1.

In this theory, the probability distribution function of a particular chain configuration, $P(\Gamma)$, and solvent density profile, $\phi_S(r, z)$, in layer z and shell r are found from a minimization of the configurational free energy of the system given by

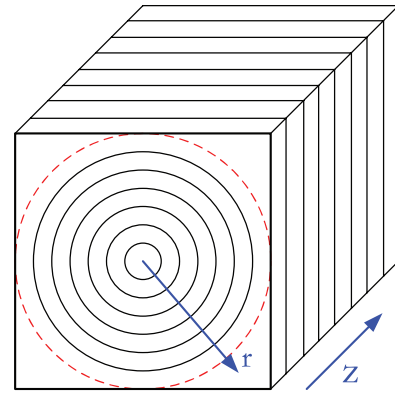


FIG. 1. Schematic diagram of the SCMFT two dimensional cylindrical fields with concentric circular shells of radius r and layers or slices of depth z . Lattice sites in the corners of the box are included with those of the last shell.

Eq. (1), subject to packing constraints,

$$\frac{F}{k_B T} = \beta N [\langle E_{inter} \rangle + \langle E_{intra} \rangle] - \frac{S}{k_B}. \quad (1)$$

A more detailed explanation can be found in a previous work.²² This minimization with constraints is carried out by introducing Lagrange multipliers, $\pi(r, z)$. The probability distribution function, $P(\Gamma)$, is obtained as

$$P(\Gamma) = \frac{\exp\{-\mathcal{H}[\Gamma]\}}{\sum_{\Gamma} \exp\{-\mathcal{H}[\Gamma]\}}, \quad (2)$$

where $\mathcal{H}[\Gamma]$ is the mean-field Hamiltonian,

$$\begin{aligned} \mathcal{H}[\Gamma] = & \chi_{TT} n_{TT}^{intra}(\Gamma) \\ & + \sum_z \sum_r \pi(r, z) \left[n_H(\Gamma, r, z) + n_T(\Gamma, r, z) \right] \\ & + \frac{\chi_{TT}}{2} \sum_z \sum_r \frac{N-1}{V(r, z)} \left[n_{n,T}(\Gamma, r, z) \langle n_T(r, z) \rangle \right. \\ & \left. + \langle n_{n,T}(r, z) \rangle n_T(\Gamma, r, z) \right], \end{aligned} \quad (3)$$

$n_H(\Gamma, r, z)$ is the number of head sites, $n_T(\Gamma, r, z)$ is the number of tail sites, and $n_{n,T}(\Gamma, r, z)$ is the number of available nearest neighbor sites in each shell, r , and layer, z , of conformation Γ . The number of chains in the systems is given by N and the volume of the shell and layer by $V(r, z)$. The angle brackets, $\langle \dots \rangle$, indicate mean field properties over the probability distribution function, $P(\Gamma)$, of the chain conformations. We define the dimensionless interaction parameter $\chi_{TT} = \beta \epsilon_{TT} = -2/T^*$, where $\beta = 1/k_B T$ and n_{TT}^{intra} is the number of intramolecular tail-tail contacts since the case where only $\epsilon_{TT} \neq 0$ is considered here.

The solvent density profile is given by

$$\phi_S(r, z) = \exp[-\pi(r, z)]. \quad (4)$$

The standard chemical potential difference between free chains, μ_N^o , and micelles of size N , μ_N^o , is calculated by the following expression:

$$\exp\left(-\frac{\mu_N^o - \mu_1^o}{k_B T}\right) \approx \frac{V \sum_{\Gamma} \exp\left(-\frac{\mathcal{H}_N(\Gamma)}{k_B T}\right) / W(\Gamma)}{N \sum_{\Gamma} \exp\left(-\frac{\mathcal{H}_1(\Gamma)}{k_B T}\right) / W(\Gamma)}, \quad (5)$$

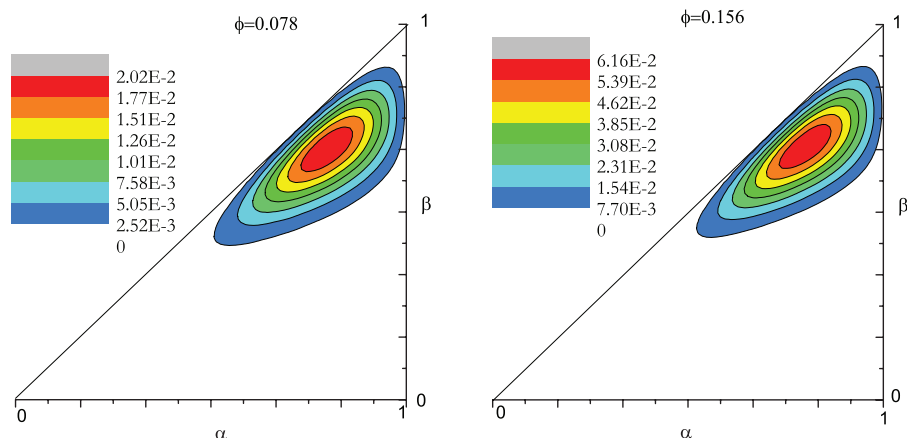


FIG. 2. Contour plots of the distribution of the α , β radii of gyration ratios, for H_4T_2 at $T^* = 4.5$ for systems with total chain volume fractions, ϕ , of 0.078 and 0.156, from Monte Carlo simulations.

where V is the simulation box volume (L^3) and $W(\Gamma)$ is the chain conformation statistical weight corresponding to the chain generation algorithm; more details can be found in a previous work.³⁰

V. RESULTS AND DISCUSSION

In this work we find that all the studied model linear surfactants, H_xT_y , form spherical micelles at low concentrations close to the CMC. However, depending on the relative head and tail chain lengths, there can be a sphere to cylinder transformation at a higher total surfactant concentration. There are different numbers of micelles depending on the simulation conditions with typically more than ten, although close to the CMC this number may be less. In addition, the cylindrical micelles are small and never span the entire simulation box and the transition from spheres to cylinders is that of a second CMC with eventual coexistence of both spherical and cylindrical micelles in a one phase system.²⁰ Preliminary work suggested that asymmetric surfactants with $x < y$ prefer cylindrical micelles at high surfactant concentration and undergo a sphere to cylinder transition, while those with $x > y$ prefer spherical micelles at all surfactant concentrations. In the case of $x = y$, calculations for longer surfactants had previously indicated that spherical micelles were always preferred but few simulations had been carried out for shorter chain lengths. The surfactants in this work have thus been divided up into three groups: $x > y$, $x < y$, and $x = y$. In the rest of this section, each of these classes will be considered in order to discover a general trend for all of these surfactants.

A. H_xT_y , $x > y$

In this section, we have carried out Monte Carlo simulations to study surfactants with a head length strictly larger than the tail length, namely, H_2T_1 , H_3T_1 , H_3T_2 , H_4T_1 , H_4T_2 , H_4T_3 . The temperatures used to study these surfactants are taken from the work by Floriano *et al.*,²³ as already commented in the Introduction. The contour plots of the ratios of the principal radii of gyration of the H_4T_2 surfactant are shown in Fig. 2 for two total chain volume fractions from

Monte Carlo simulations in a box of volume 60^3 lattice sites. All of the other surfactants have similar plots and are not given here. One can see that the peaks of these contour plots are in the spherical region (top right) for all concentration ranges considered. It is interesting to note, however, that the distribution plots, for all concentrations, show fluctuations towards cylindrical shapes (extension along the $\alpha = \beta$ axis). Similarly, the equilibrium micellar size distribution plots of chain volume fractions, ϕ , versus micelle aggregate number, N_m , for the H_4T_2 surfactant shown in Fig. 3 for three different total chain volume fractions have a single peak at aggregation numbers that correspond to spherical micelles. The plots for all the other surfactants of this section, not shown, have a similar behavior. Note that at the lowest total volume fraction the system is below the critical micelle concentration and so no micelles form and no micellar peak can be observed. This indicates that, at least for the asymmetric model surfactants studied here, on increasing the concentration of surfactants the systems choose to form additional spherical

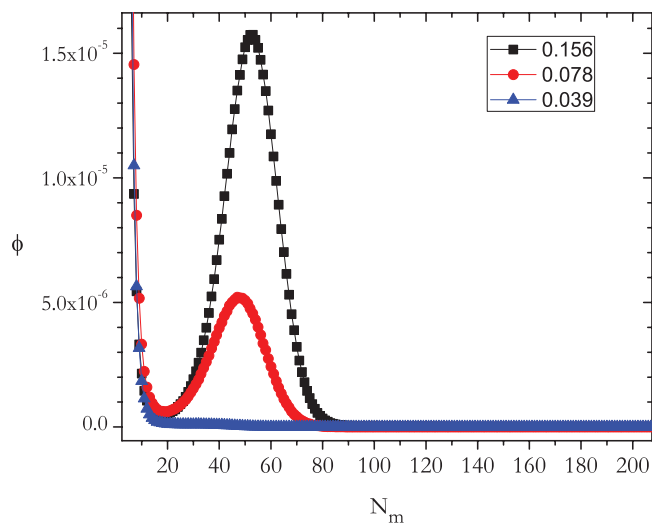


FIG. 3. Micellar size distribution plots of chain volume fraction, ϕ , versus micellar aggregation number, N_m , for H_4T_2 at $T^* = 4.5$ for systems with total chain volume fractions, of 0.039, 0.078, and 0.156, from Monte Carlo simulations.

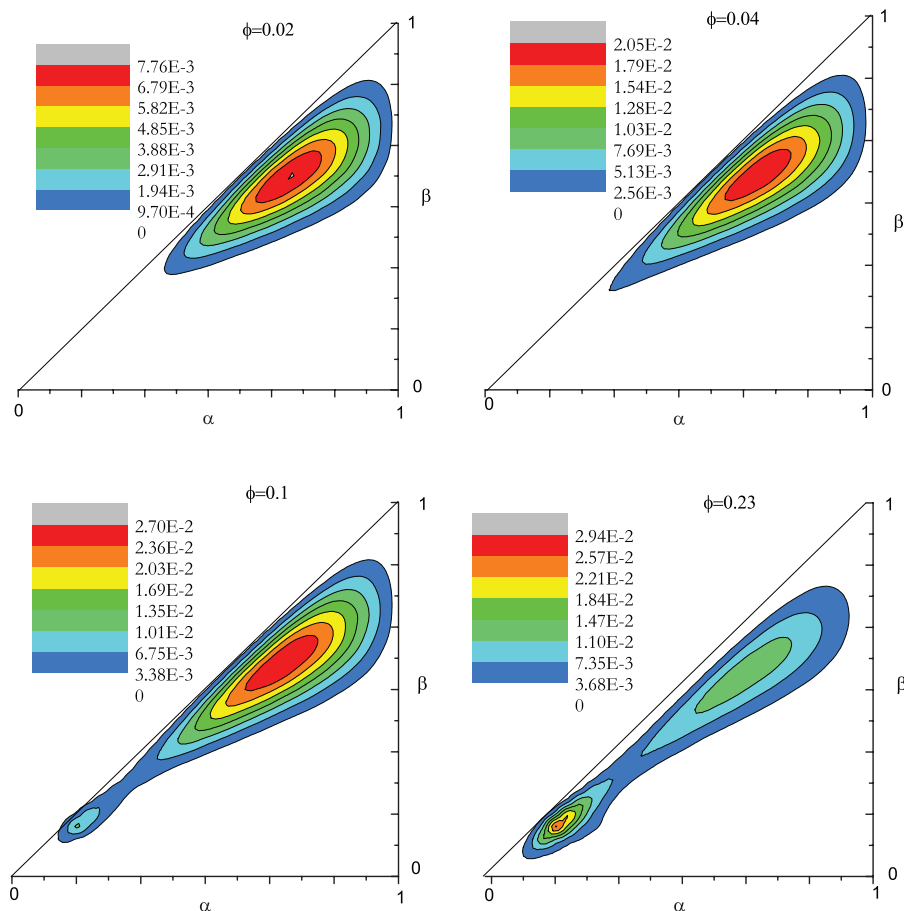


FIG. 4. Contour plots of the distribution of the α , β radii of gyration ratios, for H_4T_6 at $T^* = 9.5$ for systems with chain volume fractions, ϕ , of 0.02, 0.04, 0.10, and 0.23 from Monte Carlo simulations.

micelles of approximately the same size, instead of forming energetically less favorable larger aggregates. As a general conclusion, it can be expected that all model surfactants with a longer hydrophilic head relative to the hydrophobic tail form only spherical micelles independent of the surfactant concentration. These surfactants prefer a spherical geometry since spheres have the smallest surface area to volume ratio possible and are hence able to minimize unfavorable tail-solvent contacts.

B. H_xT_y , $x < y$

In this section, we have carried out Monte Carlo simulations to study surfactants with head lengths smaller than the tail lengths and in particular H_2T_4 , H_2T_6 , H_3T_6 , and H_4T_6 . The contour plots of the ratios of the principal radii of gyration of H_4T_6 for total surfactant volume fractions of 0.02, 0.04, 0.10, and 0.23 from Monte Carlo simulations in a box of volume 100^3 lattice sites are shown in Fig. 4. It is found that the preferred shape of the micelles at low concentrations is spherical. However, on increasing the total surfactant concentration it can be seen that cylindrical micelles also appear in the system. This can be observed by the displacement of the peak from the top right corner towards the bottom left corner in the plot. At the two higher concentrations it is also possible to see that there are two peaks in the plot, one for

the spherical micelles and an additional one for the cylindrical micelles where the cylindrical peak grows for the highest surfactant concentration in detriment to the peak for spherical micelles. All these features can be related to the underlying free energies associated with the formation of these structures which will be commented on in more detail in Sec. V C for symmetric surfactants.

The contour plot thus shows that this model surfactant, H_4T_6 , undergoes a sphere to cylinder transition through a region where spheres and cylinders coexist along with micelles of other intermediate shapes. Fig. 5 gives distribution plots of the surfactant volume fraction against the equilibrium micellar size of H_4T_6 at $T^* = 9.5$ for total surfactant concentrations of, ϕ , of 0.02, 0.04, 0.05, 0.10, and 0.23 from the same Monte Carlo simulations as for Fig. 4. At the lowest total surfactant concentration, for $\phi = 0.02$, it can be seen that there is only a very slight peak, which can be more clearly seen in the inset of the same figure. This indicates that this concentration is close to the critical micelle concentration. At these low concentrations, when micelles first start to form, they are clearly spherical as shown in Fig. 4. On increasing the overall surfactant concentration, it can be seen that a shoulder or even a second peak forms at higher aggregation numbers for the two higher total surfactant concentrations. The shoulders of the micellar size distributions are due to the existence of cylindrical micelles over the range of concentrations studied. A

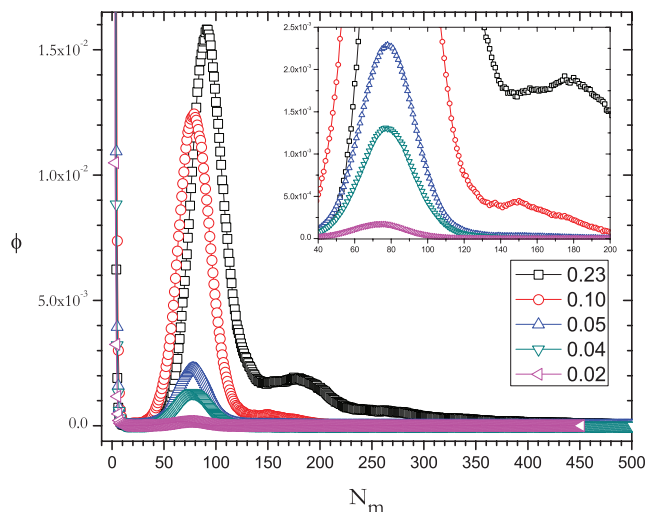


FIG. 5. Micellar size distribution plots for H_4T_6 at $T^* = 9.5$ for systems with chain volume fractions, ϕ , of 0.02, 0.04, 0.05, 0.10, and 0.23 from Monte Carlo simulations.

similar sphere to cylinder transition is also observed for the other surfactants studied here: H_2T_3 , H_2T_4 , H_3T_4 , H_2T_6 (results not shown) and the same conclusions were reached both from Monte Carlo and SCMFT results for H_3T_6 .²²

All the model surfactants, H_xT_y , with a shorter hydrophilic head relative to the hydrophobic tail studied in this work are observed to undergo a shape transition from spherical to cylindrical micelles. This tendency to form cylindrical micelles for surfactants with larger tail groups can be expected from the behavior of the well known packing parameter for micelles.³¹ This parameter is defined as v/a_0l_c , where v is the surfactant hydrophobic volume, a_0 is the optimal head group area, and l_c is the critical chain length. Spherical micelles are expected for values of the packing parameter of less than a third and non-spherical micelles for values between one third and one half. Vesicles or bilayers then follow for values between one half and one and finally inverted structures for packing parameters larger than one. For a given tail length, which effectively fixes the hydrophobic volume and critical chain length, when the head chain length is decreased

the optimal head group area also decreases and the packing parameter becomes larger. In this way, surfactants which prefer to form spherical micelles eventually give way to surfactants which prefer to form cylindrical micelles when the head group is sufficiently small.

C. H_xT_y , $x = y$

In Secs. V A and V B, it has been shown that surfactants with smaller head than tail sections (H_xT_y , $x < y$) prefer to form spherical micelles whereas surfactants which have larger tail than head sections (H_xT_y , $x > y$) have a transition from spherical to cylindrical micelles on increasing the concentration. In this section, we have carried out Monte Carlo simulations and the SCMFT for symmetrical surfactants where the tail and head sections have the same size, namely H_xT_x . Curiously, and unlike the asymmetric surfactants, the symmetric model surfactants change their behavior on increasing the chain length. The two shortest symmetric surfactants, H_1T_1 and H_2T_2 undergo a sphere to cylinder shape transition on increasing surfactant concentration. However, H_3T_3 and H_4T_4 prefer to always form spherical micelles independently of the concentration.

The contour plots of the distribution of the α and β parameters of H_2T_2 describing the ratios of the principal axis of gyration are shown in Fig. 6 from Monte Carlo simulations in a box of volume 60^3 lattice sites. At low concentrations predominantly spherical micelles are formed. However, at higher concentrations, $\phi = 0.088$, a small peak in the region of the cylindrical shapes can be observed. The formation of these two peaks is indicative of the coexistence between spherical and cylindrical micelles. At even larger concentrations, $\phi = 0.176$, the system generates mostly cylindrical micelles. Direct observations of the sphere to cylinder shape transition reveals that it occurs through a region where both spherical and cylindrical micelles coexist together with other intermediate shapes.

Furthermore, one can observe from Fig. 7 that the micellar size distributions are smooth with a peak and a noticeable shoulder at higher aggregation numbers. The presence of the cylindrical micelles can also be seen by the existence of the

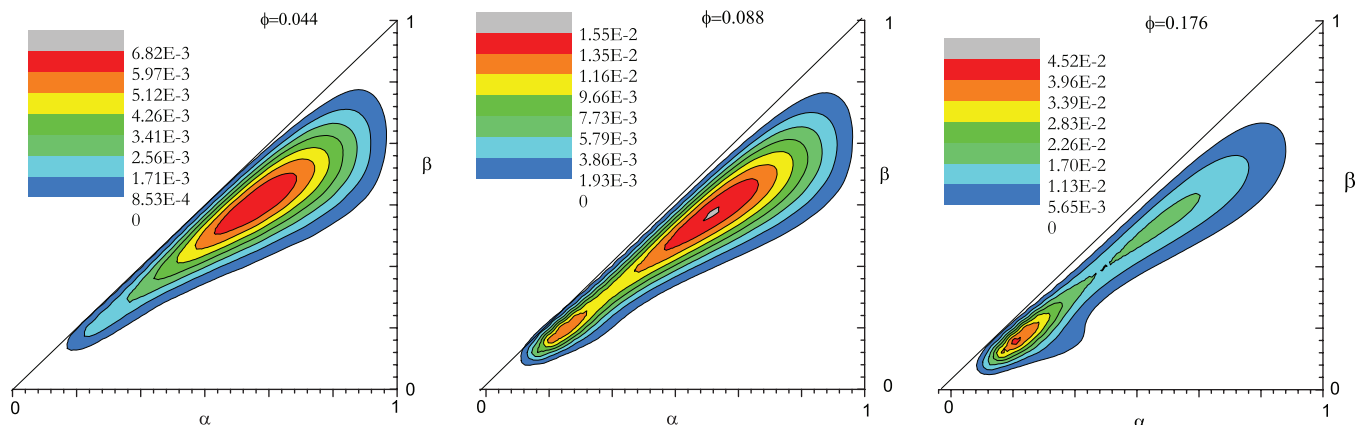


FIG. 6. Contour plots of the distribution of the α , β radii of gyration ratios, for H_2T_2 at $T^* = 4.8$ for systems with chain volume fractions, ϕ , of 0.044, 0.088, and 0.176, from Monte Carlo simulations.

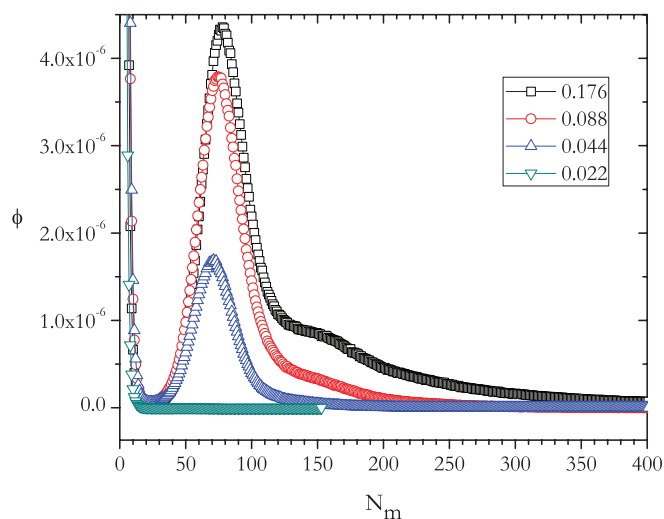


FIG. 7. Micellar size distribution plots for H_2T_2 at $T^* = 4.8$ for systems with chain volume fractions, ϕ , of 0.022, 0.044, 0.088, and 0.176, from Monte Carlo simulations.

shoulder of Fig. 7. A similar sphere to cylinder transition is observed for model surfactant H_1T_1 (results not shown).

Fig. 8 shows the contour plots of the ratios of the principal radii of gyration for the symmetric surfactant H_3T_3 from Monte Carlo simulations in a box of volume 100^3 lattice sites. Unlike the shorter H_1T_1 and H_2T_2 surfactants, only spherical micelles can be observed. It can be seen that the peaks of these contour plots correspond to the spherical region of the contour plot for all concentrations considered, although with some fluctuations towards cylindrical shapes (extension along the $\alpha = \beta$ axis). Similarly, the equilibrium micellar size distribution of H_3T_3 , as shown in Fig. 9, is found to be smooth with a single peak at aggregation numbers that correspond to stable spherical micelles. This shows that for these model surfactants, on increasing the total number of surfactants, the system prefers to form more spherical micelles of the same size, instead of aggregating the additional surfactants into less energetically favorable larger micelles. The same behavior was found for the H_4T_4 surfactant in a previous paper²² where only spherical micelles were found to form.

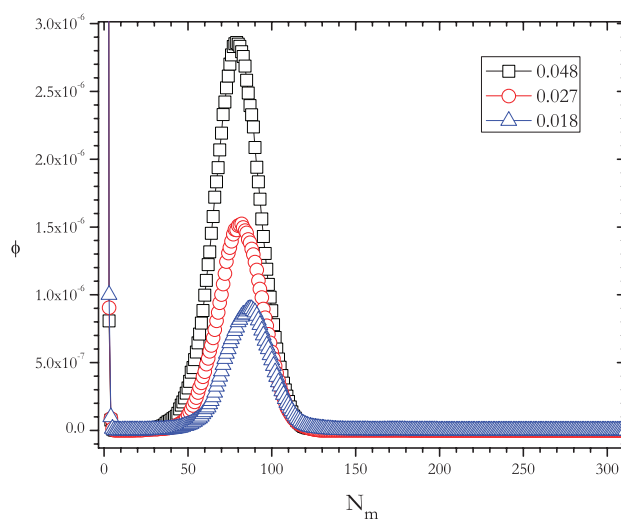


FIG. 9. Micellar size distribution plots for H_3T_3 at $T^* = 5$ for systems with chain volume fractions, ϕ , of 0.018, 0.027, and 0.048, from Monte Carlo simulations.

The shape transition characteristics described above have also been studied using the Single Chain Mean Field Theory. In Fig. 10 a plot of the standard chemical potential difference between free chains, μ_1^o , and micelles of size N , μ_N^o , from Eq. (5) versus the number of surfactants in the micelle N_m is given. The first minimum (at $N_m \approx 55$) corresponds to a stable spherical micelle and the second (at $N_m \approx 160$) to a cylindrical micelle with two hemispherical ends while the maximum (at $N_m \approx 115$) corresponds to a prolate spheroid. The same trend is obtained for SCMFT calculations for H_1T_1 (results not shown). The existence of these minimums and maximums with relatively small differences in free energy is indicative of a possible shape transition, in this case of micelles that undergo a sphere to cylinder transition and a detailed analysis of this can be found elsewhere.²² These results are in agreement with the observations from the Monte Carlo simulation and help support the conclusion that the H_1T_1 and H_2T_2 surfactants indeed undergo a transformation from spherical to cylindrical micelles on increasing the overall surfactant concentration. The standard chemical potential difference versus

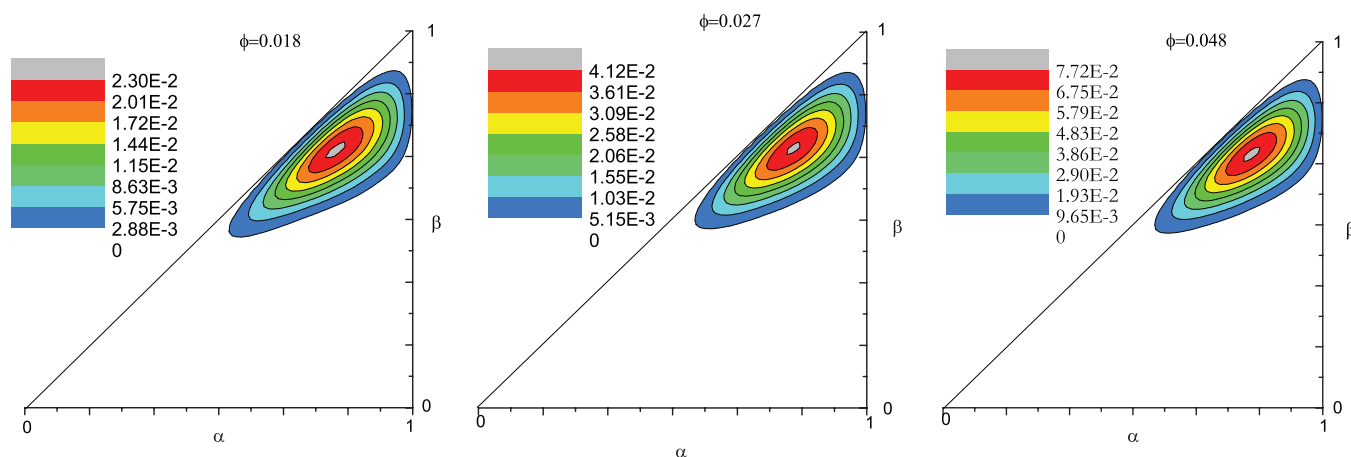


FIG. 8. Contour plots of the distribution of the α , β radii of gyration ratios, for H_3T_3 at $T^* = 5$ for systems with chain volume fractions, ϕ , of 0.018, 0.027, and 0.048, from Monte Carlo simulations.

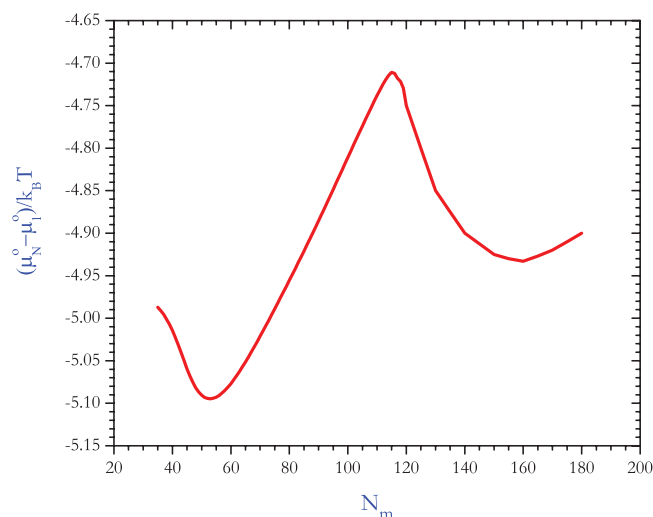


FIG. 10. The standard chemical potential difference, $(\mu_N^o - \mu_1^o)/k_B T$, versus micellar aggregation number, N_m , of H_2T_2 , at dimensionless temperature $T^* = 4.8$ from two dimensional Single Chain Mean Field Theory calculations.

aggregation number for H_3T_3 is shown in Fig. 11. Unlike the H_2T_2 surfactant, only one minimum is observed in this case at $N_m \approx 45$. This minimum corresponds to a spherical micelle and no cylindrical micelles are formed, only larger and less favorable spherical micelles. A similar observation has also been made for the H_4T_4 surfactant.²² The observation that only spherical micelles are preferred for H_3T_3 and H_4T_4 surfactants is once again consistent with the Monte Carlo simulations and gives further weight to this conclusion.

VI. CONCLUSIONS

In this work, the concentration induced morphological transformations of a series of linear model nonionic surfactants H_xT_y have been explored. Our Monte Carlo simulations lead to insight into the self-assembling process and give direct observations of the shape of micelles formed and the shape transitions they undergo. Asymmetric surfactants with

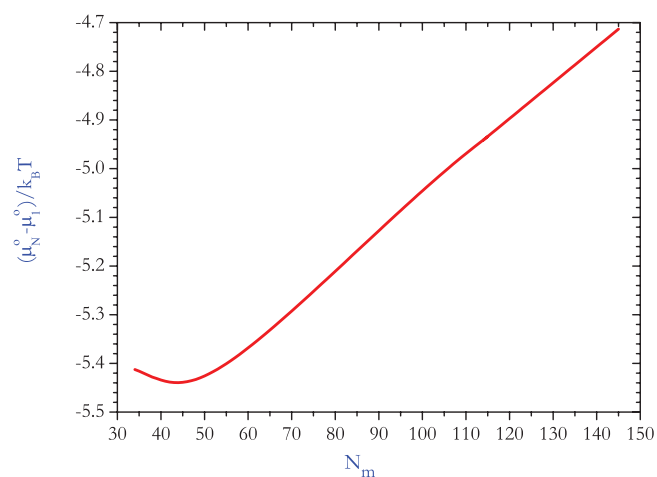


FIG. 11. The standard chemical potential difference, $(\mu_N^o - \mu_1^o)/k_B T$, versus micellar aggregation number, N_m , of H_3T_3 , at dimensionless temperature $T^* = 5.0$ from two dimensional Single Chain Mean Field Theory calculations.

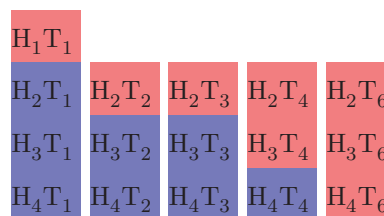


FIG. 12. Sphere versus sphere to cylinder transition for linear H_xT_y surfactants. Blue cells represent surfactants that prefer to form spherical micelles and red cells represent surfactants that undergo a sphere to cylinder shape transition.

longer hydrophilic heads than hydrophobic tails ($x > y$) prefer to form spherical micelles independent of the total surfactant concentration. On the other hand, asymmetric surfactants with shorter head groups than the tail groups ($x < y$) form spherical micelles at lower concentration and elongate into cylindrical micelles on increasing the total surfactant concentration. Finally, symmetric model surfactants H_xT_y , where $x = y$, are found to form micelles of different geometries depending on their chain length. The shortest of these surfactants, H_1T_1 and H_2T_2 , show a sphere to cylinder shape transition. However, longer symmetric surfactants such as H_3T_3 and H_4T_4 have been observed to form only spherical micelles. This detail has been confirmed by SCMFT calculations where the same tendency was found when the standard chemical potential difference was calculated.

The morphological characteristics of the micelles of all the surfactants studied in the present work are summarized in Fig. 12. The surfactants not shown of the same series of H_xT_2 , and H_xT_4 have been found to have a phase transition rather than forming micelles in the work by Floriano *et al.*²³ As can be seen for a series of surfactants of a given tail length (the columns of Fig. 12), on reducing the number of head groups the micelles pass from being always spherical to having a sphere to cylinder shape transition, and finally have only a phase transition rather than the formation of micelles. In the case of the series of surfactants with just one tail group, H_xT_1 , the shortest surfactant, H_1T_1 , is still found to form micelles rather than a phase transition, although a sphere to cylinder transition is observed. This behavior follows the tendency expected from the packing parameter of Israelachvili,³¹ $v/a_o l_c$, where by shortening the head length the head area, a_o , is reduced while the tail volume and length remain the same. This effectively causes the packing parameter to increase and at some given point cylindrical micelles become more favorable than spherical ones. The sphere to cylinder shape transition appears to always anticipate the phase transition and is indicative of the proximity of a true second macroscopic phase rather than the formation of micelles. Indeed, as the head group becomes smaller compared to the tail, the chain loses its amphiphilic qualities and becomes effectively dominated by the solvophobic interaction leading to a second phase.

ACKNOWLEDGMENTS

The authors would like to thank Professor M. A. Floriano for his suggestion to study the shape transitions of these systems.

- ¹C. A. Palma, M. Cecchini, and P. Samori, *Chem. Soc. Rev.* **41**, 3713 (2012).
- ²P. Debye and E. W. Anacker, *J. Phys. Colloid Chem.* **55**, 644 (1951).
- ³J. C. Eriksson and S. Ljunggren, *J. Chem. Soc. Faraday Trans. 2* **81**, 1209 (1985).
- ⁴J. Molina-Bolívar, J. Aguiar, J. M. Peula-García, and C. C. Ruiz, *J. Phys. Chem. B* **108**, 12813 (2004).
- ⁵A. Rodríguez, M. del Mar Graciani, K. Bitterman, A. T. Carmona, and M. L. Moya, *J. Colloid Interface Sci.* **313**, 542 (2007).
- ⁶S. P. Denkova, L. V. Lokeren, I. Verbruggen, and R. Willem, *J. Phys. Chem.* **112**, 10935 (2008).
- ⁷W. Lin, C. Zheng, X. Wan, D. Liang, and Q. Zhou, *Macromolecules* **43**, 5405 (2010).
- ⁸S. J. Lee and M. J. Park, *Langmuir* **26**, 17827 (2010).
- ⁹P. Kaewsaiha, K. Matsumoto, and H. Matsuoka, *Langmuir* **23**, 9162 (2007).
- ¹⁰H. Xuehao, H. Liang, and C. Pan, *Phys. Rev. E* **63**, 031804 (2001).
- ¹¹T. Zehl, M. Wahab, H. J. Mögel, and P. Schiller, *Langmuir* **22**, 2523 (2006).
- ¹²T. Zehl, M. Wahab, R. Schmidt, P. Schiller, and H. Mögel, *J. Mol. Liq.* **147**, 178 (2009).
- ¹³P. H. Nelson, G. C. Rutledge, and T. A. Hatton, *J. Chem. Phys.* **107**, 10777 (1997).
- ¹⁴Y. Termonia, *J. Polym. Sci.* **40**, 890 (2002).
- ¹⁵M. Kenward and M. D. Whitmore, *J. Chem. Phys.* **116**, 3455 (2002).
- ¹⁶Y. Sheng, X. Yang, N. Yanab, and Y. Zhu, *Soft Matter* **9**, 6254 (2013).
- ¹⁷S. J. Marrink, D. P. Tieleman, and A. E. Mark, *J. Phys. Chem. B* **104**, 12165 (2000).
- ¹⁸S. Fujiwara, T. Itoh, M. Hashimoto, and R. Horiuchi, *J. Phys. Chem.* **130**, 144901 (2009).
- ¹⁹S. May and A. Ben-Shaul, *J. Phys. Chem.* **105**, 630 (2001).
- ²⁰Z. A. Al-Anber, J. Bonet-Avalos, M. A. Floriano, and A. D. Mackie, *J. Chem. Phys.* **118**, 3816 (2003).
- ²¹A. B. Jódar-Reyes and F. A. M. Leermakers, *J. Phys. Chem. B* **110**, 6300 (2006).
- ²²A. G. Daful, J. B. Avalos, and A. D. Mackie, *Langmuir* **28**, 3730 (2012).
- ²³A. Z. Panagiotopoulos, M. A. Floriano, and S. K. Kumar, *Langmuir* **18**, 2940 (2002).
- ²⁴R. G. Larson, *J. Chem. Phys.* **83**, 2411 (1985).
- ²⁵A. D. Mackie, K. Onur, and A. Z. Panagiotopoulos, *J. Chem. Phys.* **104**, 3718 (1996).
- ²⁶A. Ben-Shaul, W. M. Gelbart, and I. Szleifer, *J. Chem. Phys.* **83**, 3597 (1985).
- ²⁷I. Szleifer, A. Ben-Shaul, and W. M. Gelbart, *J. Chem. Phys.* **83**, 3612 (1985).
- ²⁸A. D. Mackie, A. Z. Panagiotopoulos, and I. Szleifer, *Langmuir* **13**, 5022 (1997).
- ²⁹A. G. Daful, "Microscopic modeling of the self assembly of surfactants: Shape transitions and critical micelle concentrations," Ph.D. thesis (Universitat Rovira i Virgili, Tarragona, Spain, 2011).
- ³⁰Z. A. Al-Anber, J. Bonet-Avalos, and A. D. Mackie, *J. Chem. Phys.* **122**, 104910 (2005).
- ³¹J. Israelachvili, *Intermolecular and Surface Forces*, 7th ed. (Academic Press, California, USA, 1998).